Three-Dimensional Guidance Law for Landing on a Celestial Object

Der-Cherng Liaw,* Chiz-Chung Cheng,†
and Yew-Wen Liang‡
National Chiao Tung University,
Hsinchu 30010, Taiwan, Republic of China

Introduction

As space vehicle technology develops, the rendezvous of a space vehicle with a space station or a celestial object becomes possible and imminent. Many rendezvous guidance strategies for landing on an asteroid or the docking of two vehicles have been studied recently. The rendezvous problems of two space vehicles in two dimensions were presented in Refs. 1 and 2. Under similar dynamical equations, the rendezvous of a space vehicle with an asteroid was discussed in Refs. 3 and 4. However, the existing studies tended to neglect the combined impact of atmosphere and gravity. The Viking Lander descent to Mars through an unknown atmosphere density profile, winds, and terrain characteristics was described in Ref. 5. Autonomous spacecraft navigation and control for a comet landing with model error and the effects of environmental disturbances was analyzed by Monte Carlo simulation in Ref. 6. The rendezvous with a celestial object usually consists of three successive phases[3]: 1) cruise or transfer to the vicinity of the celestial body, 2) approach, and 3) maneuvers near the celestial body. This Note is concerned with maneuver near the celestial body by using the generalized three-dimensional model with the effects of both gravity and atmospheric drag. Moreover, in this Note, the unmodeled perturbing forces such as solar radiation pressure and nonspherical gravitational effects are treated as disturbances.[7] These perturbing forces usually cause periodic variations[8] and will be formulated as trigonometric functions.

The main goal of this Note is, from a theoretic point of view, to propose a new landing guidance law for ensuring the vehicle landing on the celestial body in a finite time and satisfying the landing constraint in the terminal phase when the space vehicle approaches a celestial body. That is, $\boldsymbol{v} \to 0$ as $r \to r_a$, where r_a denotes the celestial radius. By properly selecting the desired trajectory, the landing process is transformed into a tracking problem. The variable structure control (VSC) technique is then applied to the design of a tracking control law. By the construction of a time-varying boundary layer, the tracking performance is shown to be achieved at an exponential convergence rate. Moreover, the modified guidance law attained is continuous and alleviates the classical chattering drawback of the VSC control scheme. An illustrative example is also presented to demonstrate the use of the results.

Landing Control Problem

The rendezvous kinematics model in vectorial form are given by[4]

$$\dot{\boldsymbol{r}} = \boldsymbol{v}, \qquad \dot{\boldsymbol{v}} = \boldsymbol{a} - (\mu/r^3)\boldsymbol{r} + \boldsymbol{f} + \boldsymbol{d} \tag{1}$$

Here, $\boldsymbol{r}, \boldsymbol{v}, \boldsymbol{a}, \boldsymbol{f}$, and $\boldsymbol{d}$ denote the position, velocity, and applied, drag, and disturbance accelerations, respectively, and μ is the gravitational constant times the mass of the asteroid. The velocity $\boldsymbol{v}$ in the spherical coordinate system (r, θ, ϕ) can be expressed as[9]

$$\boldsymbol{v} = \dot{r}\boldsymbol{e}_r + r\dot{\theta}\cos\phi\,\boldsymbol{e}_\theta + r\dot{\phi}\boldsymbol{e}_\phi \tag{2}$$

where r is the distance from the spacecraft to the celestial object, θ and ϕ are the azimuth and pitch angles with respect to the celestial body, and $\boldsymbol{e}_r$, $\boldsymbol{e}_\theta$, and $\boldsymbol{e}_\phi$ are unit vectors along the coordinate vectors. An atmospheric model with varying density would likely be described by a combination of the outgassing type[10] and the hydrostatic effects represented as an exponential model.[7] The drag acceleration $\boldsymbol{f}$ is, hence, assumed to have the form

$$\boldsymbol{f} = -\beta(\boldsymbol{v}/\|\boldsymbol{v}\|)\|\boldsymbol{v}\|^2\left(w_1 r^{-2} + w_2 e^{-kr}\right) \tag{3}$$

Here, $\beta > 0$ denotes the drag coefficient, and w_i is a weighting constant for $i = 1, 2$.

Design of Smooth Guidance Control Law

Let $\boldsymbol{x} = [\boldsymbol{x}_1^T, \boldsymbol{x}_2^T]^T$, where $\boldsymbol{x}_1 = [x_1 \;\; x_2 \;\; x_3]^T = [r \;\; \theta \;\; \phi]^T$ and $\boldsymbol{x}_2 = [x_4 \;\; x_5 \;\; x_6]^T = [\dot{r} \;\; \dot{\theta} \;\; \dot{\phi}]^T$. The system equations (1) then become

$$\dot{\boldsymbol{x}}_1 = \boldsymbol{x}_2 \tag{4}$$

$$\dot{\boldsymbol{x}}_2 = A(\boldsymbol{x}) + B(\boldsymbol{x})\boldsymbol{u} + B(\boldsymbol{x})\boldsymbol{d} \tag{5}$$

where

$$A(\boldsymbol{x}) = \begin{bmatrix} x_1x_6^2 + x_1x_5^2\cos^2 x_3 - \mu/x_1^2 \\ 2x_5x_6\tan x_3 - 2x_4x_5/x_1 \\ -2x_4x_6/x_1 - x_5^2\cos x_3\sin x_3 \end{bmatrix}$$

$$- \beta\sqrt{x_4^2 + (x_1x_5\cos x_3)^2 + (x_1x_6)^2}\cdot\left(w_1r^{-2} + w_2e^{-kr}\right)$$

$$\times \begin{bmatrix} x_4 \\ x_1x_5\cos x_3 \\ x_1x_6 \end{bmatrix} \tag{6}$$

$$B(\boldsymbol{x}) = \begin{bmatrix} 1 & 0 & 0 \\ 0 & 1/x_1\cos x_3 & 0 \\ 0 & 0 & 1/x_1 \end{bmatrix}, \qquad \boldsymbol{d} = \begin{bmatrix} d_1 \\ d_2 \\ d_3 \end{bmatrix}, \qquad \boldsymbol{u} = \begin{bmatrix} a_r \\ a_\theta \\ a_\phi \end{bmatrix} \tag{7}$$

We impose the following assumption on the disturbance.

Assumption 1: The uncertainty $\boldsymbol{d}$ is uniformly bounded with respective to $\boldsymbol{x}$ and t, and there exists some $w(\boldsymbol{x})$ function such that

$$\|B(\boldsymbol{x})\boldsymbol{d}\| \le w(\boldsymbol{x}) \qquad \text{for all } t \text{ and } \boldsymbol{x} \tag{8}$$

For the landing problem, we need to have $r \to r_a$ in a finite time. To achieve this goal, let $\boldsymbol{x}_d = [x_{d1} \;\; x_{d2} \;\; x_{d3}]^T$ be the desired trajectory of $\boldsymbol{x}_1$ where x_{d1}, x_{d2}, and x_{d3} are all twice differentiable functions of t, and x_{d1} is chosen so that $x_{d1} \to r_a - \delta$, for some $\delta > 0$, as $t \to \infty$. The landing process then becomes a trajectory tracking problem. Denote the tracking error vector as $\boldsymbol{e} = \boldsymbol{x}_1 - \boldsymbol{x}_d$. The design objective is then to synthesize a control law such that the closed-loop system having the error vector $\boldsymbol{e}$ approaches zero. The system equations (4) and (5) can then be rewritten as

$$\begin{bmatrix} \dot{\boldsymbol{e}} \\ \dot{\xi} \end{bmatrix} = \begin{bmatrix} \xi \\ A(\xi, \boldsymbol{e}, \boldsymbol{x}_d) + B(\xi, \boldsymbol{e}, \boldsymbol{x}_d)\boldsymbol{u} + B(\xi, \boldsymbol{e}, \boldsymbol{x}_d)\boldsymbol{d} - \ddot{\boldsymbol{x}}_d^2 \end{bmatrix} \tag{9}$$

where $\xi = \dot{\boldsymbol{e}}$, $\boldsymbol{x}_1 = \boldsymbol{x}_d + \boldsymbol{e}$ and $\boldsymbol{x}_2 = \dot{\boldsymbol{x}}_d + \dot{\boldsymbol{e}}$. According to the design of a VSC-type controller, the control input is divided into two parts. One is the so-called equivalent control, and the other is compensation control. Also, such a design is known to consist of three steps: 1) choose an appropriate sliding surface S to be function of system states, 2) design the equivalent control for the nominal system such that the origin of the reduced model of the system on the sliding surface $S = 0$ is asymptotically stable, and 3) implement an extra control effort to compensate for possible uncertainties and/or disturbances and steer all of the system states, which are not on the sliding

Received 5 April 1999; revision received 1 December 1999.

*Associate Professor, Department of Electrical and Control Engineering; dcliaw@cc.nctu.edu.tw.

†Assistant Scientist, CHUNG-SHAN Institute of Science and Technology.

‡Associate Professor, Department of Electrical and Control Engineering.

surface, to the sliding surface. From the theory of VSC, the origin of the system can then be guaranteed to be asymptotically stable. Following the VSC design procedure, we choose a time-varying sliding surface S as

$$S(\boldsymbol{e}, \xi) = \xi + M\boldsymbol{e} = 0 \tag{10}$$

where $M \in \mathbb{R}^{3\times 3}$ is a positive-definite matrix. The VSC-type controller has the form

$$u = u_{\text{eq}} + u_N \tag{11}$$

where u_{eq} denotes the equivalent control for the nominal system (i.e., the system Eqs. (4) and (5) with $\boldsymbol{d} = 0$), and u_N is the control to be designed to compensate for disturbances and/or uncertainties. First, we design the equivalent control u_{eq} for the nominal system to guarantee the stability of the reduced model on the sliding surface. Note that the input-related matrix $B(\boldsymbol{x})$ is nonsingular and

$$\dot{S} = -\ddot{\boldsymbol{x}}_d + M\xi + A(\xi, \boldsymbol{e}, \boldsymbol{x}_d) + B(\xi, \boldsymbol{e}, \boldsymbol{x}_d)u \tag{12}$$

for $\boldsymbol{d} = 0$. The equivalent control u_{eq} can then be chosen as

$$u_{\text{eq}} = B^{-1}(\xi, \boldsymbol{e}, \boldsymbol{x}_d)[\ddot{\boldsymbol{x}}_d - M\xi - A(\xi, \boldsymbol{e}, \boldsymbol{x}_d)] \tag{13}$$

which leads to $\dot{S} = 0$. From Eq. (10), the reduced system model on the sliding surface, that is, $S = 0$, becomes

$$\dot{\boldsymbol{e}} = -M\boldsymbol{e} \tag{14}$$

It is clear that the tracking error vector $\boldsymbol{e}$ exponentially decays to zero because M is a positive-definite matrix. This leads to the results of $\boldsymbol{x}_1 \to \boldsymbol{x}_d$ as time t increase for any system state lying on the sliding surface $S = 0$. Next, we design the control u_N to compensate for the disturbance $\boldsymbol{d}$ and to drive all of the system states, which are not on the sliding surface $S = 0$, to enter the sliding surface. For any system state not lying on the sliding surface, that is, $S(\boldsymbol{e}, \xi) \neq 0$, we have

$$S^T\dot{S} = S^T[A(\xi, \boldsymbol{e}, \boldsymbol{x}_d) + B(\xi, \boldsymbol{e}, \boldsymbol{x}_d)(u_{\text{eq}} + u_N) + M\boldsymbol{x}_2 - \ddot{\boldsymbol{x}}_d - M\dot{\boldsymbol{x}}_d$$
$$+ B(\xi, \boldsymbol{e}, \boldsymbol{x}_d)\boldsymbol{d}] = S^T[B(\xi, \boldsymbol{e}, \boldsymbol{x}_d)u_N + B(\xi, \boldsymbol{e}, \boldsymbol{x}_d)\boldsymbol{d}] \tag{15}$$

Let u_N be given by

$$u_N = -[w(\boldsymbol{x}) + \eta]B^{-1}(\xi, \boldsymbol{e}, \boldsymbol{x}_d)g(S) \tag{16}$$

where $w(\boldsymbol{x})$ is defined in Eq. (8), $\eta > 0$ and

$$g(S) = 2S/(\|S\| + \epsilon e^{-\gamma t}) \tag{17}$$

Here, $\epsilon > 0$ and $\gamma > 0$ are selected by the designer and γ is interpreted as the convergence rate to the sliding surface, which will become clear in Eq. (22). Note that the control law u_N is continuous everywhere and that $u_N = 0$ on the sliding surface.

For the case $\|S(t)\| \geq \epsilon e^{-\gamma t}$ and $u = u_{\text{eq}} + u_N$, we have

$$\begin{aligned} S^T\dot{S} &= S^T[B(\xi, \boldsymbol{e}, \boldsymbol{x}_d)u_N + B(\xi, \boldsymbol{e}, \boldsymbol{x}_d)\boldsymbol{d}] \\ &\leq -2(w(\boldsymbol{x}) + \eta)\frac{\|S\|^2}{\|S\| + \epsilon e^{-\gamma t}} + w(\boldsymbol{x}) \cdot \|S\| \\ &\leq -(w(\boldsymbol{x}) + \eta) \cdot \|S\| + w(\boldsymbol{x}) \cdot \|S\| \\ &\leq -\eta \cdot \|S\| \end{aligned} \tag{18}$$

Thus, $(\boldsymbol{e}, \xi)$ will reach the time-varying boundary layer

$$\Gamma(\boldsymbol{e}, \xi, t) = \{\boldsymbol{e} \mid \|S(\boldsymbol{e}, \xi, t)\| \leq \epsilon e^{-\gamma t}\} \tag{19}$$

in a finite time with time less than $S(\boldsymbol{e}_0, \xi_0)/\eta$. This then implies that the boundary layer $\Gamma(\boldsymbol{e}, \xi, t)$ is an attractive invariant set for $S(\boldsymbol{e}, \xi, t)$. Now, we consider the behavior of $(\boldsymbol{e}, \xi) \in \Gamma(\boldsymbol{e}, \xi, t)$. Let

$$\boldsymbol{z}(t) = \dot{\boldsymbol{e}} + M\boldsymbol{e} \tag{20}$$

where $\boldsymbol{e}$ satisfies Eq. (9). It follows that

$$\boldsymbol{e}(t) = e^{-Mt}\boldsymbol{e}(0) + \int_0^t e^{-M(t-\tau)}\boldsymbol{z}(\tau)\,\mathrm{d}\tau \tag{21}$$

Because M is a positive-definite matrix, we have $e^{-Mt}\boldsymbol{e}(0) \to 0$ as $t \to \infty$, where the initial state is assumed to lie within $\Gamma(\boldsymbol{e}, \xi, t)$. Moreover, because $(\boldsymbol{e}, \xi) \in \Gamma(\boldsymbol{e}, \xi, t)$, from Eq. (19), we have $\|\boldsymbol{z}\| \leq \epsilon e^{-\gamma t}$ and

$$\begin{aligned} &\left\| \int_0^t e^{-M(t-\tau)}\boldsymbol{z}(\tau)\,\mathrm{d}\tau \right\| \\ &\quad \leq \|e^{-Mt}\| \cdot \int_0^t \|e^{M\tau}\| \cdot \|\boldsymbol{z}(\tau)\|\,\mathrm{d}\tau \\ &\quad \leq e^{-\lambda_{\min}(M)t} \cdot \int_0^t e^{\lambda_{\max}(M)\tau} \cdot \epsilon e^{-\gamma\tau}\,\mathrm{d}\tau \\ &\quad \leq \begin{cases} e^{-\lambda_{\min}(M)t} \cdot \epsilon t & \text{if} \quad \gamma = \lambda_{\max}(M) \\ e^{-\lambda_{\min}(M)t}\left(\epsilon/[\lambda_{\max}(M) - \gamma]\left\{e^{[\lambda_{\max}(M)-\gamma]t} - 1\right\}\right) & \text{if} \quad \gamma \neq \lambda_{\max}(M) \end{cases} \end{aligned} \tag{22}$$

where $\lambda_{\min}(\cdot)$ and $\lambda_{\max}(\cdot)$ denote the smallest and the largest eigenvalues of a matrix, respectively. Hence, we have

$$\int_0^t e^{-M(t-\tau)}\boldsymbol{z}(\tau)\,\mathrm{d}\tau \to 0$$

exponentially as $t \to \infty$ when $\gamma > \lambda_{\max}(M) - \lambda_{\min}(M)$. From Eq. (21), we have the tracking error vector $\boldsymbol{e}(t) \to 0$ exponentially as $t \to \infty$. This implies that $\boldsymbol{x}_1 \to \boldsymbol{x}_d$ as $t \to \infty$. The next theorem follows readily from the preceding derivations.

Theorem 1: Consider system (4) and (5). Let $\boldsymbol{x}_d$ be a given trajectory for landing. Suppose the disturbance $\boldsymbol{d}$ satisfies conditions (8). Then, under the control law $u = u_{\text{eq}} + u_N$, where u_{eq} and u_N are given by Eqs. (13) and (16), respectively, with $M > 0$ and $\gamma > \lambda_{\max}(M) - \lambda_{\min}(M)$, the landing performance can be achieved at an exponential convergence rate. Moreover, the control law is continuous and alleviates the chattering behavior.

Simulation Results

In this section, we present an example to illustrate the use of the main result. In this example, the desired output is chosen as $\boldsymbol{y} = [r_a + (r_o - r_a)\exp(-t/10) - \delta, \theta_f, \phi_f]^T$, where δ is a positive parameter to ensure that the vehicle lands on the celestial body in finite time. Now, consider the case of a spacecraft landing on a spherical asteroid with radius $r_a = 10$ km. Initial conditions for the numerical study are adopted from Ref. 4 and drag coefficients are from Ref. 10. Other system parameters are chosen to satisfy landing requirements and desired transient response. The system parameters are then given as $r_o = 200$ km, $\theta_f = 0.5$ rad, $\phi_f = 0.5$ rad, $\theta_o = 0.2$ rad, $\phi_o = 0.2$ rad, $\dot{r}_o = -20$ km/h, $\dot{\theta}_o = 0.2$ rad/h and $\dot{\phi}_o = 0.2$ rad/h, $\mu = 4000$ km^3/h^2, $k = 0.1$, $\beta = 0.02$, $\eta = 2$, $\epsilon = 1$, $\delta = 0.1$ km, and $\gamma = 0.01$. Moreover, the disturbances are assumed to be $d_1 = 0.1\sin x_3$, $d_2 = 0.5\cos x_3$, and $d_3 = 0.2\cos x_3$, whereas the weighting factors are $w_1 = 1$ and $w_2 = 1$. Numerical simulations are given in Fig. 1. In Fig. 1, the solid line shows the norm of the error function $\boldsymbol{e}$ with scale multiplied by 10^2, the dashed line depicts the effect of gravity, and the dotted line exhibits the norm of air drag with scale multiplied by 10^4. It is observed from Fig. 1 that the tracking performance is achieved at an exponential rate. The

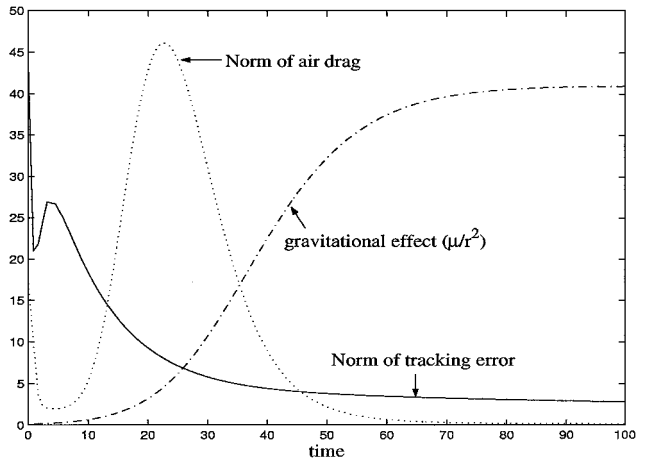

Fig. 1 Norm of tracking error e and the effects of air drag and gravity.

amount of acceleration has been used to denote the required energy consumption for the landing process.[1,3,4] In this study, we adopt the same idea to employ the norm of the control input u for expressing the required energy for landing. The relationship between control effort and mass of propellant m_p required for landing can be expressed as[11] $\int \|u\| \, dt \propto \ell n[m_0/(m_0 - m_p)]$, where m_0 is the initial vehicle mass.

Conclusion

We have considered the rendezvous of a space vehicle with a celestial object. The study included the effects of drag and disturbance. By employing the variable structure control technique, a continuous guidance law has been proposed to guarantee the tracking performance and alleviate the classical chattering drawback. The tracking performance has the property of exponential convergence rate, which can be assigned by the designer. Finally, an illustrative example was presented to demonstrate the use of the main results.

Acknowledgment

This research was supported by the National Science Council, Taiwan, Republic of China under Grant NSC 88-2212-E-009-022.

References

[1]Yuan, P. J., and Hsu, S. C., "Rendezvous Guidance with Proportional Navigation," *Journal of Guidance, Control, and Dynamics*, Vol. 17, No. 2, 1993, pp. 409–411.

[2]Shaohua, Y., "Terminal Spacecraft Coplanar Rendezvous Control," *Journal of Guidance, Control, and Dynamics*, Vol. 18, No. 4, 1995, pp. 838–842.

[3]Guelman, M., "Guidance for Asteroid Rendezvous," *Journal of Guidance, Control, and Dynamics*, Vol. 14, No. 5, 1991, pp. 1080–1083.

[4]Guelman, M., and Harel, D., "Power Limited Soft Landing on an Asteroid," *Journal of Guidance, Control, and Dynamics*, Vol. 17, No. 1, 1994, pp. 15–20.

[5]Robert, N. I., "Guidance and Control System Design of the Viking Planetary Lander," *Journal of Guidance, Control, and Dynamics*, Vol. 1, No. 3, 1978, pp. 189–196.

[6]Lafontaine, J. D., "Autonomous Spacecraft Navigation and Control for Comet Landing," *Journal of Guidance, Control, and Dynamics*, Vol. 15, No. 3, 1992, pp. 567–576.

[7]Myint-U. T., "Effect of Oblateness and Drag on Equatorial Orbits with Small Eccentricities," *Journal of Spacecraft and Rockets*, Vol. 5, No. 1, 1968, pp. 123–125.

[8]Wertz, J. R., and Larson, W. J., *Space Mission Analysis and Design*, Kluwer Academic, Norwell, MA, 1991, Chap. 6, pp. 123–129.

[9]Yang, C. D., and Yang, C. C., "Analytical Solution of Three-Dimensional Realistic True Proportional Navigation," *Journal of Guidance, Control, and Dynamics*, Vol. 19, No. 3, 1996, pp. 569–577.

[10]Persen, L. N., "Motion of a Satellite with Friction," *Jet Propulsion*, Vol. 28, No. 11, 1958, pp. 750–752.

[11]Das, B. M., Kassimali, A., and Sami, S., *Engineering Mechanics: Dynamics*, Richard D. Irwin, 1994, Chap. 5, pp. 217–221.

Setpoint Generation for Constant-Velocity Motion of Space-Based Scanners

Rebecca A. Masterson*
Massachusetts Institute of Technology, Cambridge, Massachusetts 02139
William E. Singhose†
Georgia Institute of Technology, Atlanta, Georgia 30332
and
Warren P. Seering‡
Massachusetts Institute of Technology, Cambridge, Massachusetts 02139

I. Introduction

THE performance of flexible spacecraft that contain constant-velocity scanning payloads is degraded by vibration that corrupts the desired motion. The vibration disturbances can come from numerous sources including gravity gradients, attitude control reaction wheels,[1–3] jet propulsion systems,[4–6] thermoelastic deformation,[7,8] fluid sloshing,[9] and payload-payload interactions.[10] There are a number of possible ways to deal with these corrupting disturbances such as using vibration isolation systems,[11] concurrently designing the structure and controller,[12] and generating vibration-reducing motion setpoints.[13] Scanners often need to perform rapid changes in velocity and direction to achieve high cycle throughput. These setpoint changes can induce vibration that corrupts the constant-velocity portion of the scanning cycle. In this case, the scanner motion corrupts its own signal.

Consider the position profile shown in Fig. 1. The profile has several regions where the desired scanning velocity is constant ($\pm v_1$). These constant-velocity regions are separated by high-velocity regions ($\pm v_2$) and changes in direction. This type of command is used with systems that perform constant-velocity scanning over sub regions of their workspace. Between these regions, the system attempts to move rapidly to the next scanning region. If the system has flexibility, then the response will contain vibration superimposed on the constant-velocity motion.

Regions 1–4 of Fig. 1 represent the position ranges over which the mass is required to move at the constant velocity, v_1, while performing the scanning operation. An auxiliary goal is to move the system as slowly as possible over the scan regions while keeping the total duration of the cycle fixed. The slow scanning velocity allows the sensor more time to make a measurement and, consequently, the accuracy is improved.

The profile shown in Fig. 1 was chosen because it is representative of high-performance scanning profiles. There is much to gain by using high-velocity motions between the scanning regions. If the system traveled at a single constant velocity over both the scanning and nonscanning regions, the slowest scan velocity it could use (given the position set points in Fig. 1) while still completing a cycle in the desired time (0.25 s in this example) would be 6.24 cm/s. However, if the nonscan velocity v_2 were infinite, the system could traverse the scanning regions as slowly as 2.4 cm/s while still completing the cycle in 0.25 s.

The ideal profile, then, has the smallest possible scanning velocity v_1 and infinite nonscanning velocity v_2. This profile allots the maximum time available for the scanning process. The time available for

Received 14 June 1999; revision received 25 April 2000; accepted for publication 26 April 2000.

*Research Assistant, Department of Mechanical Engineering. Member AIAA.

†Assistant Professor, Department of Mechanical Engineering. Member AIAA.

‡Professor, Department of Mechanical Engineering.